

Supporting Information

Kim et al. 10.1073/pnas.1216401109

SI Text

Cells Maintained in the Turbidostat Exhibit Similar F_t Behavior Compared with Cells Transferred to the Fast Repetition Rate Fluorometer. The PSI FMT 150 photobioreactor allows for the measurement of F_t within the growing chamber. However, these data have poor signal to noise because of convection from bubbling. Nonetheless, the general trends observed in Fig. S5 are consistent with the fast repetition rate (FRR) fluorometry results in Fig. 4 and Fig. S4. Fluorescence is significantly more quenched after the light–dark (LD) transition and less quenched after the DL transition.

The origin and maximum fluorescence traces in Fig. 4 exhibit an underlying baseline with a positive slope. This finding is mirrored in the variable fluorescence yield measurements. Given that such a feature is not present in F_t measurements in the turbidostat (Fig. S5), we attribute the sloping baselines of Fig. 4 to the physiological adaptation of the cells during the 20-h measurement period. Note that the baseline is present in both L and D periods of the experiment. This finding suggests that this behavior is not the result of photoinhibition, which contributes to the photoinhibitory fluorescence quenching (qI) component of nonphotochemical quenching (qN) (1). qI contributions can be excluded given that the actinic light source in FRR fluorometry experiments ($60 \mu\text{E m}^{-2} \text{s}^{-1}$) is less intense than the light source in the turbidostat ($100 \mu\text{E m}^{-2} \text{s}^{-1}$).

Changes in Fluorescence Quenching After the LD and DL Transitions Are the Result of Photosystem II Activity. qN resulting from changes in the thylakoid membrane proton gradient is denoted qE (1). To study the effects of qE after the LD and DL transitions, the blue actinic source in the FRR fluorometer sample chamber was replaced with a 735-nm near-IR LED; 735 nm only excites photosystem I (PSI) and does not affect photosystem II (PSII). During 735-nm illumination, cyclic electron transfer around PSI is active, thus enhancing the thylakoid membrane proton gradient and enabling photophosphorylation (2). As shown in Fig. S6, no significant change in fluorescence quenching occurs after either LD or DL transition. This observation suggests that the dramatic changes in fluorescence quenching observed in Fig. 4

and Figs. S4 and S5 are photochemical in nature and not the result of qE.

Increased Fluorescence Quenching During the Dark Period Is the Result of the Acceptor Side of PSII. Data in Fig. 4 and Fig. S4 represent average values over five single turnover flashes (STFs). Full data for each STF number are shown in Fig. S7. During the periods when the actinic light is on, chlorophyll (Chl) fluorescence is not dependent on STF number. However, during the dark period, origin and maximum Chl fluorescence levels are more quenched during the first STF. We attribute this observation to donor- and acceptor-side contributions to photochemical quenching (qP). On the donor side of PSII, Chl fluorescence is most quenched by the dark-stable S_1 intermediate of the PSII water-oxidizing complex (3). On the acceptor side, after a 2-min dark adaptation, the primary electron acceptor, Q_A , is more likely to be oxidized.

The STF number dependence of fluorescence quenching in Fig. S7 does not show indications of oscillations. Given the cyclic nature of the water-oxidizing complex turnover cycle, significant contributions of donor-side qP would be present as a damped period four oscillatory pattern in the variable yield of Chl fluorescence with minimum yield on the third STF (3). F_v/F_m values in Fig. S7 are lower on the fourth and fifth STFs than the third STF. We rationalize this behavior by suggesting that acceptor-side contributions of qP are more significant than S-state quenching. In other words, the relative population of Q_A to Q_A^- decreases during the five STFs in this FRR fluorometry experiment.

Fluorescence Quenching Does Not Change After the LD Transition When the Plastoquinone Pool Is Fully Reduced. Introducing the cyt b_6f inhibitor 2,5-dibromo-3-methyl-6-isopropyl-p-benzoquinone (DBMIB) to illuminated cells results in a fully reduced plastoquinone (PQ) pool (PSII reduces PQ, which cannot be reoxidized by cyt b_6f) (Scheme S2). The LD transition was specifically probed in the presence of DBMIB as shown in Fig. S8. No change in fluorescence quenching is observed when the PQ pool is fully reduced. This observation supports our prior assertion that the primary quenching mechanism involves acceptor-side contributions to qP (i.e., Q_A).

1. Krause G, Jahns P (2004) Non-photochemical energy dissipation determined by chlorophyll fluorescence quenching: Characterization and function. *Chlorophyll a Fluorescence, Advances in Photosynthesis and Respiration*, eds Papageorgiou GC, Govindjee (Springer, Berlin), pp 463–495.
2. Skizim NJ, Ananyev GM, Krishnan A, Dismukes GC (2012) Metabolic pathways for photobiological hydrogen production by nitrogenase- and hydrogenase-containing unicellular cyanobacteria Cyanotherce. *J Biol Chem* 287(4):2777–2786.

3. Shinkarev V (2004) Photosystem II: Oxygen evolution and chlorophyll a fluorescence induced by multiple flashes. *Chlorophyll a Fluorescence, Advances in Photosynthesis and Respiration*, eds Papageorgiou GC, Govindjee (Springer, Berlin), pp 197–229.

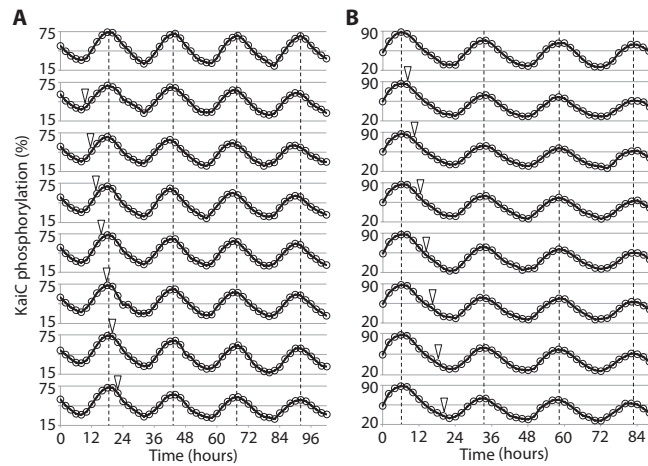


Fig. S1. The effect of dithionite addition in the in vitro oscillator mixture. (A) Dithionite (300 μ M final concentration) was added on the phosphorylation phase of KaiC in 2-h intervals (open triangle). The dotted lines were aligned on the peak positions of a control in vitro oscillator mixture to which no Q_0 was added to aid comparisons of the timing of peaks in each reaction. (B) Same as A except that dithionite was added on the dephosphorylation phase.

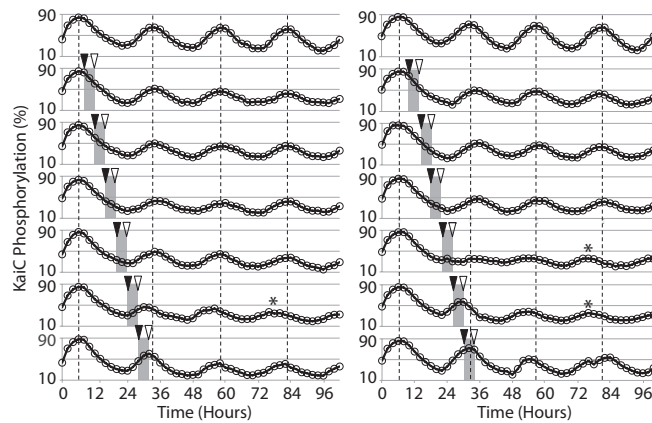


Fig. S2. The effect of the 4-h addition of oxidized Q_0 . Phase shift was monitored by addition of 4-h oxidized Q_0 with every 2-h interval. The oxidized Q_0 was added at the solid triangle, and dithionite was added at the open triangle to reduce Q_0 . The observed phase shift was marked with an asterisk.

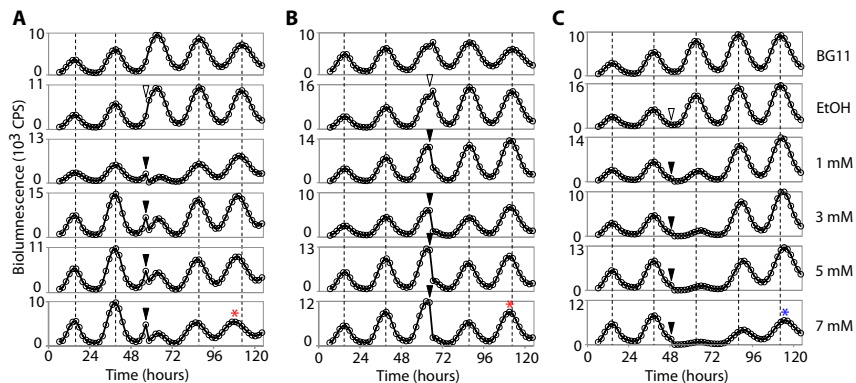


Fig. S3. The phase response with Q_0 addition in vivo at constant light. The oxidized Q_0 was added at circadian times (A) 9, (B) 17, and (C) 24. For the control experiment, ethanol was added at the open triangle. The oxidized Q_0 concentrations applied to all experiments are shown to the right to C. The phase advance (red asterisk) and delay (blue asterisk) peaks used on Fig. 2 are marked on the graph.

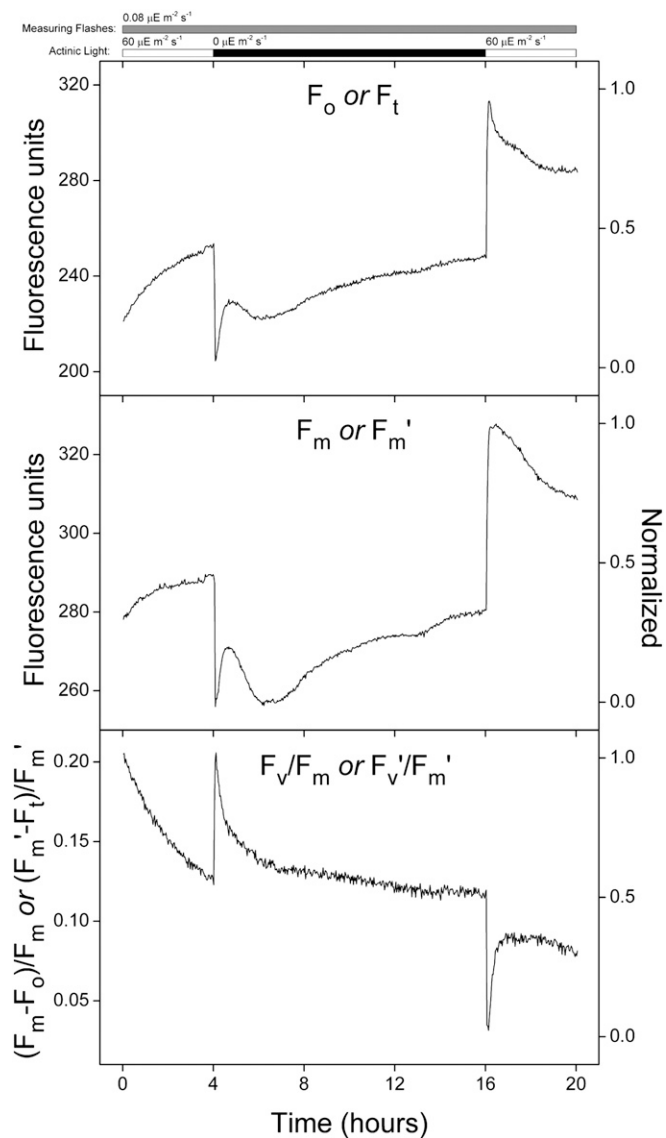


Fig. S4. Full FRR fluorescence traces measured during the simulated diurnal cycle as described in Fig. 4.

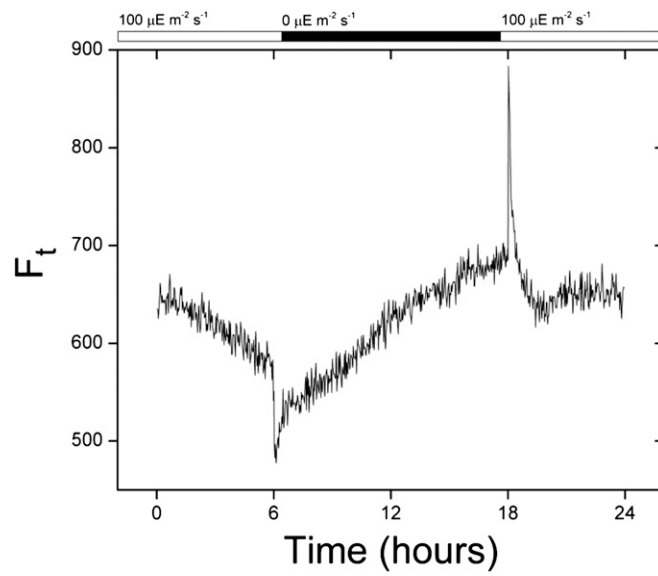


Fig. 55. Instantaneous fluorescence during the diurnal cycle as measured within the turbidostat by pulse amplitude modulation (PAM) fluorometry.

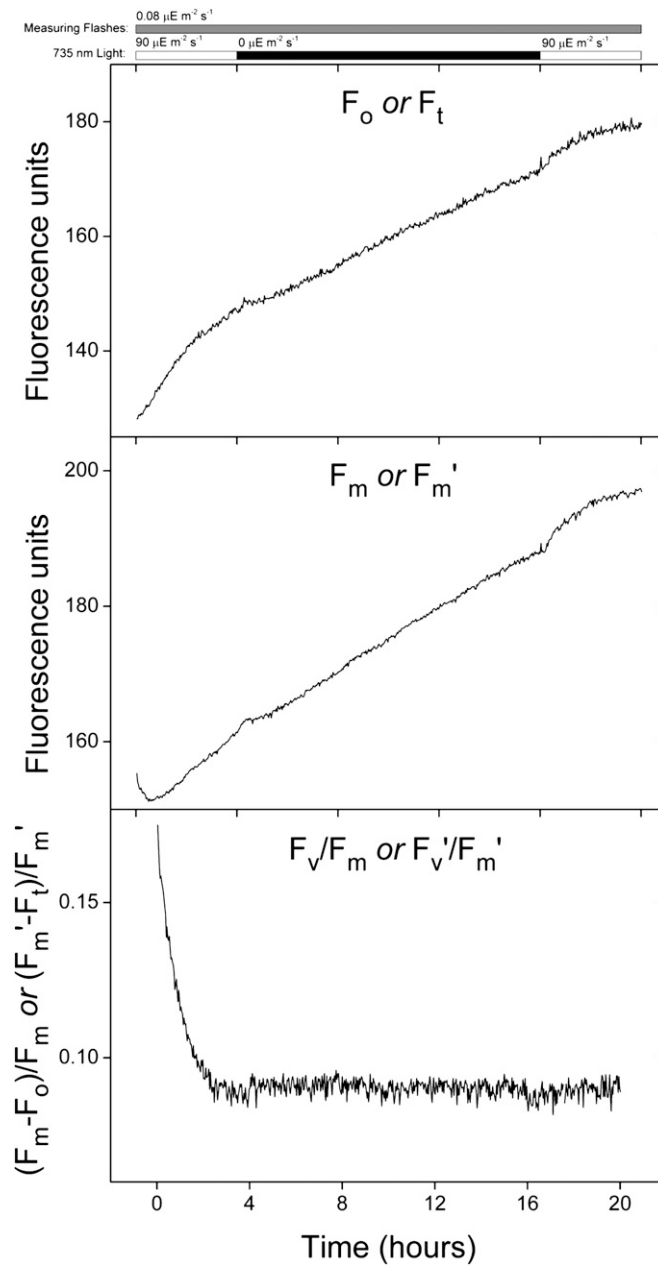


Fig. S6. FRR fluorescence traces during a modified diurnal cycle in which only PSI is activated during the light periods; 735-nm light ($90 \mu\text{E m}^{-2} \text{s}^{-1}$) illuminated the sample during hours 0–4 and 16–20.

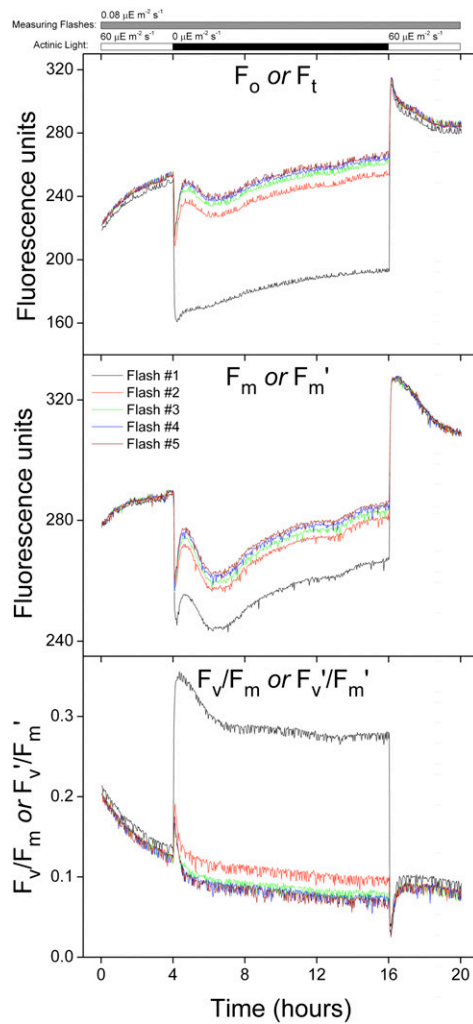


Fig. S7. Changes in FRR fluorescence parameters based on STF number.

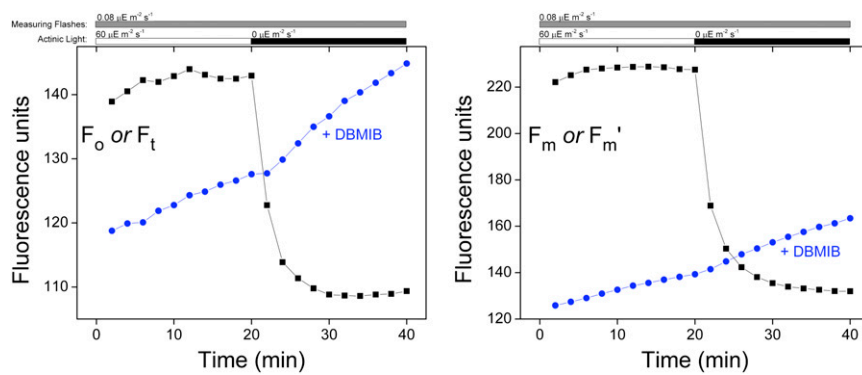
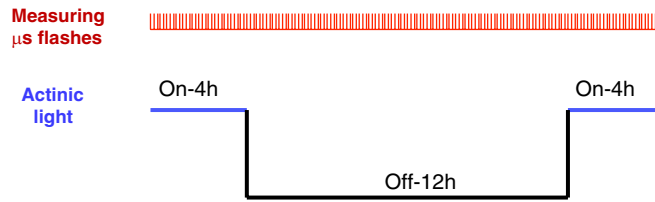
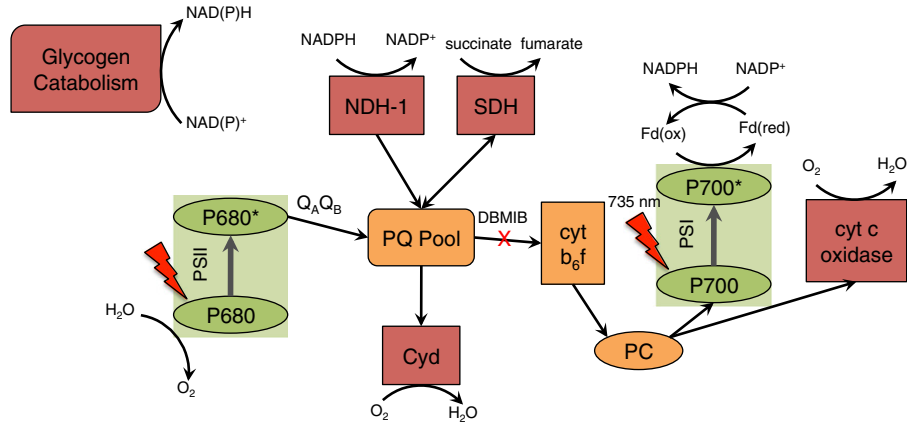


Fig. S8. Origin and maximum fluorescence before and after the LD transition in the presence of DBMIB. The sample was illuminated with blue actinic light during the first 20 min.



Scheme S1. FRR fluorometry flash protocol.



Scheme S2. Key pathways involved in photosynthetic and respiratory reduction and oxidation of the PQ pool in *Synechococcus elongatus* PCC 7942. Green, photosynthesis only; red, respiration only; orange, both processes. Modified from Vermaas (1) and Skizim et al. (2).

1. Vermaas W (2001) *Photosynthesis and Respiration in Cyanobacteria*. *Encyclopedia of Life Sciences* (Wiley, New York), pp 1–7.
2. Skizim NJ, Ananyev GM, Krishnan A, Dismukes GC (2012) Metabolic pathways for photobiological hydrogen production by nitrogenase- and hydrogenase-containing unicellular cyanobacteria Cyanothecae. *J Biol Chem* 287(4):2777–2786.